

Young Do Koo,¹ Jin Woo Choi,¹ Myungjin Kim,² Sehyun Chae,³ Byung Yong Ahn,¹ Min Kim,¹ Byung Chul Oh,⁴ Daehee Hwang,³ Jae Hong Seol,² Young-Bum Kim,^{5,6} Young Joo Park,¹ Sung Soo Chung,¹ and Kyong Soo Park^{1,6}



SUMO-Specific Protease 2 (SEN2) Is an Important Regulator of Fatty Acid Metabolism in Skeletal Muscle

Diabetes 2015;64:2420–2431 | DOI: 10.2337/db15-0115

Small ubiquitin-like modifier (SUMO)-specific proteases (SENPs) that reverse protein modification by SUMO are involved in the control of numerous cellular processes, including transcription, cell division, and cancer development. However, the physiological function of SENPs in energy metabolism remains unclear. Here, we investigated the role of SEN2 in fatty acid metabolism in C2C12 myotubes and in vivo. In C2C12 myotubes, treatment with saturated fatty acids, like palmitate, led to nuclear factor- κ B-mediated increase in the expression of SEN2. This increase promoted the recruitment of peroxisome proliferator-activated receptor (PPAR) δ and PPAR γ , through desumoylation of PPARs, to the promoters of the genes involved in fatty acid oxidation (FAO), such as carnitine-palmitoyl transferase-1 (CPT1b) and long-chain acyl-CoA synthetase 1 (ACSL1). In addition, SEN2 overexpression substantially increased FAO in C2C12 myotubes. Consistent with the cell culture system, muscle-specific SEN2 overexpression led to a marked increase in the mRNA levels of CPT1b and ACSL1 and thereby in FAO in the skeletal muscle, which ultimately alleviated high-fat diet-induced obesity and insulin resistance. Collectively, these data identify SEN2 as an important regulator of fatty acid metabolism in skeletal muscle and further implicate that muscle SEN2 could be a novel therapeutic target for the treatment of obesity-linked metabolic disorders.

Insulin resistance precedes the development of type 2 diabetes mellitus and is characterized by impaired

insulin-dependent glucose metabolism in metabolically active tissues, such as skeletal muscle, liver, and adipose tissues. Among these tissues, skeletal muscle is one of the major sites that expend glucose. There is a negative relationship between muscle triglyceride levels and insulin sensitivity (1–4), and insulin sensitivity is reduced by fatty acid overload in cultured myocytes (5). Several trials to increase fatty acid oxidation (FAO) or to limit fat storage in muscle have been shown to improve obesity-induced insulin resistance (6–9), which can be applied for the treatment of insulin resistance.

Peroxisome proliferator-activated receptors (PPARs) are members of the nuclear receptor superfamily and comprise three isoforms: PPAR α , PPAR δ , and PPAR γ . All are involved in lipid metabolism and glucose homeostasis, although they show different tissue distributions and physiological roles (10). PPAR δ is expressed ubiquitously in all tissues, and its agonists facilitate FAO in skeletal muscle via PPAR γ coactivator (PGC)1 α (11). PPAR γ is highly expressed in adipocytes and plays an essential role in adipogenesis (12).

Small ubiquitin-like modifier (SUMO) is conjugated to a variety of proteins and modulates their localization, stability, and interaction with other proteins (13,14). SUMO modification (sumoylation) is involved in the control of various cellular processes, including cell cycle progression, gene expression, and signal transduction (15,16). Sumoylation can be reversed by the action of SUMO-specific cysteine proteases (SENPs). Six mammalian SENP

¹Department of Internal Medicine, Seoul National University College of Medicine, Seoul, Korea

²School of Biological Sciences, Seoul National University, Seoul, Korea

³School of Interdisciplinary Bioscience and Bioengineering, Pohang University of Science and Technology, Pohang, Korea

⁴Lee Gil Ya Cancer and Diabetes Institute, Gachon University, Incheon, Korea

⁵Division of Endocrinology, Diabetes and Metabolism, Department of Medicine, Beth Israel Deaconess Medical Center and Harvard Medical School, Boston, MA

⁶Department of Molecular Medicine and Biopharmaceutical Sciences, Graduate School of Convergence Science and Technology, College of Medicine, Seoul National University, Seoul, Korea

Corresponding author: Kyong Soo Park, kspark@snu.ac.kr or Sung Soo Chung, suschung@snu.ac.kr.

Received 26 January 2015 and accepted 27 February 2015.

This article contains Supplementary Data online at <http://diabetes.diabetesjournals.org/lookup/suppl/doi:10.2337/db15-0115/-/DC1>.

© 2015 by the American Diabetes Association. Readers may use this article as long as the work is properly cited, the use is educational and not for profit, and the work is not altered.

family members have been identified, and they have different subcellular locations and substrate specificity (17–20). SENPs also play important roles in the control of various cellular events. Knockout of either *SENP1* or *SENP2* results in embryonic lethality (21–23), suggesting that the regulation of sumoylation is essential for developmental processes. Moreover, disruption of SUMO homeostasis contributes to the development and progression of prostate cancer, in which *SENP1* and *SENP3* are critically involved (24–26). It is also known that *SENP2* desumoylates Mdm2, an ubiquitin E3 ligase of p53, and contributes to the control of p53-mediated processes (27). However, relatively little is known about the role of SENPs in the regulation of energy metabolism. Recent studies have shown that *SENP2* represses glycolysis and reprograms glucose metabolism in cancer cells and *SENP1* overexpression increases mitochondrial biogenesis in myotubes (28,29).

Several transcription factors involved in metabolic regulation, such as PPAR γ and PGC1 α , are known to serve as targets for sumoylation (30,31). We have recently shown that *SENP2* desumoylates PPAR γ and dramatically increases the activity of PPAR γ (32). Interestingly, the sumoylation status of PPAR γ selectively regulates the expression of some PPAR γ target genes in myotubes: desumoylation of PPAR γ increases the mRNA level of fatty acid translocase (CD36) but not of adipose differentiation-related protein (ADRP), although both are upregulated by PPAR γ agonists. Based on these reports, we hypothesized that *SENP2* is involved in metabolic regulation in skeletal muscle. In this study, we investigated the potential role of *SENP2* in the regulation of fatty acid metabolism in skeletal muscle by using a cultured cell system and a genetically engineered animal model.

RESEARCH DESIGN AND METHODS

Materials

Expression vectors for PPARs, SUMO-1, SENPs, ubiquitin conjugating enzyme 9 (UBC9), and PPAR response element-thymidine kinase-luciferase (*PPRE-TK-Luc*) reporter vector (*pPPRE-TK-Luc*) were prepared as previously described (32). An expression vector for PGC1 α was obtained from Dr. Gang Xu (The Chinese University of Hong Kong, Hong Kong). Reporter vectors for *SENP2* were also generated: (–1980)-*Luc*, (–868)-*Luc*, and (–157)-*Luc* (33). Mutations in the nuclear factor- κ B (NF- κ B) binding site of (–157)-*Luc* were generated by substituting GGG (–70 to –68 bp) with CTC. Adenovirus containing the human *SENP2* expression construct (Ad-*SENP2*) was prepared as previously described (32). All small interfering (si)RNAs were purchased from Dharmacon except for PPAR γ siRNA (Invitrogen). Polyclonal antibody against *SENP2* was produced using the peptide representing amino acid 317–335 of mouse *SENP2* as an epitope (Abclon, Korea).

Cell Culture and Transfection

C2C12 myoblasts were maintained in DMEM supplemented with 10% FBS (Invitrogen). Differentiation was

induced using DMEM containing 2% horse serum (Invitrogen) for 4 days. Transfection of plasmids was performed using Lipofectamin with Plus Reagent (Invitrogen), and siRNAs were transfected using RNAiMAX (Invitrogen).

RNA Preparation and Real-Time PCR

Total RNAs were isolated by using TRIzol (Invitrogen), and real-time PCR was performed using SYBR-master mix (Takara) and ABI 7500 real-time PCR system (Applied Biosystems). Nucleotide sequences of the primers are shown in Supplementary Table 1.

Measurement of Fatty Acid Oxidation

For measurement of FAO, muscle tissues or cells were homogenized in an ice-cold mitochondria isolation buffer (250 mmol/L sucrose, 10 mmol/L Tris-HCl, and 1 mmol/L EDTA). The lysates were incubated for 2 h with 0.2 mmol/L [1-¹⁴C]palmitate. ¹⁴CO₂ and ¹⁴C-labeled acid-soluble metabolites were quantified using a liquid scintillation counter. Each radioactivity was normalized by protein amount of each lysate.

Electrophoretic-Mobility Shift Assays

The probe was labeled with biotin and incubated with nuclear extracts from C2C12 myotubes treated with palmitate for 24 h in the binding buffer (LightShift Chemiluminescent electrophoretic-mobility shift assay [EMSA] kit). The sequences of the probe and competitors are shown in Supplementary Table 1.

Chromatin Immunoprecipitation Coupled With Quantitative PCR

After cross-linking and DNA fragmentation, nuclear extracts were subjected to immunoprecipitation with antibodies against PPAR α , PPAR δ , PPAR γ , PGC1 α , and control IgG. The sequences of primers are listed in Supplementary Table 1.

Microarray

Gene expression of C2C12 cells was profiled using MouseRef-8-v2-BeadChip (Illumina). The array was scanned using a BeadStation 500 System (Illumina).

Animals and Metabolic Analyses

All aspects of animal care and experimentation were conducted in accordance with the National Institutes of Health *Guide for the Care and Use of Laboratory Animals* (NIH publ. no. 85-23, revised 1996). The mice were DXA scanned using a LUNAR Prodigy scanner with software version 8.10 (GE Healthcare). The levels of free fatty acid and triglyceride were measured (BioVision). For electron microscopical analysis, thin muscle sections were prepared and examined using a transmission electron microscope (JEM-1400) at 80 Kv.

Statistical Analysis

Statistical analysis was performed using SPSS version 12.0 (SPSS Inc.). Statistical significance was tested using the Mann-Whitney *U* test. A *P* value <0.05 was considered statistically significant.

RESULTS

Palmitate Elevates the Expression of SENP2 in C2C12 Myotubes

In an attempt to identify the factor(s) that regulates SENP2 expression, C2C12 myotubes were treated with various metabolites, hormones, and cytokines. The expression of SENP2 mRNA was not significantly changed upon treatment with insulin, glucose, interleukin-6, or tumor necrosis factor- α (Supplementary Fig. 1). However, it was markedly increased by treatment with palmitate (Fig. 1A), and this increase occurred in dose- and incubation time-dependent fashions, respectively (Fig. 1B and C). Increase in the SENP2 protein levels by palmitate was also confirmed (Supplementary Fig. 1B). On the other hand, unsaturated fatty acids, such as oleate, linoleate, and eicosapentaenoic acid, showed little or no effect on the SENP2 mRNA levels (Fig. 1A). In addition, the expression of SENP1, another SENP, was not influenced by any of the tested fatty acids, including palmitate (Supplementary Fig. 1C), suggesting that palmitate specifically regulates the expression of SENP2 in myotubes.

SENP2 Expression Is Regulated by Palmitate-Induced NF- κ B Activation

Palmitate is known to induce NF- κ B activation (34,35). It has also been shown that toll-like receptor 4 (TLR4) and MyD88 are responsible for palmitate-induced NF- κ B activation (34,36,37). Treatment with pyrrolidine dithiocarbamate, a selective NF- κ B inhibitor, abrogated palmitate-mediated increase in the mRNA level of SENP2 (Fig. 1D). Consistently, knockdown of NF- κ B by specific siRNAs (confirmed at Supplementary Fig. 2A) completely inhibited the effect of palmitate on the SENP2 mRNA level (Fig. 1E). Moreover, knockdown of TLR4 or MyD88 (confirmed at Supplementary Fig. 2B) led to suppression of palmitate-induced expression of SENP2 mRNA (Fig. 1F). These results suggest that the increase in the SENP2 mRNA level is mediated by palmitate-induced NF- κ B activation via TLR4 and MyD88.

For determination of whether the promoter of the mouse *SENP2* gene has a *cis*-acting element for NF- κ B-mediated regulation, its 5'-flanking region was serially deleted and inserted into a *Luc* reporter vector. Palmitate treatment led to three- to fourfold increase in the *Luc* activity upon transfection of the constructs having the regions from -1980, -868, and -157 to +93 bp (Fig. 1G). Furthermore, a potential NF- κ B-binding sequence was found to locate at ~70 bp upstream of the transcription start site (as shown at Fig. 1H) and mutations of the sequence abrogated palmitate-induced promoter activity (Fig. 1G). To confirm this finding, we performed EMSA by using nuclear extracts of C2C12 myotubes. Palmitate treatment led to a dramatic increase in a binding with a biotin-labeled probe containing the putative NF- κ B-binding sequence (Fig. 1H, lane 3), and this increased binding could be abolished by treatment with the same but unlabeled probe (lane 4) as well as with the unlabeled consensus NF- κ B-binding sequence (lane 6), but not with an oligonucleotide having the mutated sequence (lane 5).

Furthermore, the band was supershifted by addition of anti-NF- κ B antibody (lane 7). These results suggest that the *SENP2* promoter has a *cis*-acting element for palmitate-induced NF- κ B binding.

SENP2 Promotes Palmitate-Mediated Increase in the Expression of Acyl-CoA Synthetase 1, Carnitine-Palmitoyl Transferase 1b, and UCP3

Long-chain acyl-CoA synthetase (ACSL)1 and carnitine-palmitoyl transferase (CPT)1 are known to play a critical role in FAO (38,39). In addition, uncoupling protein (UCP)3 has also been shown to augment FAO (40,41). Henceforth, we referred to ACSL1, CPT1b, and UCP3 as FAO-associated enzymes. Palmitate treatment led to an increase in the mRNA levels of FAO-associated enzymes in a dose-dependent fashion (Fig. 2A). Furthermore, knockdown of SENP2 (Supplementary Fig. 3) suppressed the increase in the mRNA levels of all three proteins (Fig. 2B). Consistently, palmitate-stimulated FAO was abrogated by SENP2 knockdown (Fig. 2C). These results suggest that SENP2 plays a crucial role in the control of FAO under conditions with overloaded saturated fatty acids.

Overexpression of SENP2 Increases FAO Primarily By Upregulating the Expression of FAO-Associated Enzymes

We performed mRNA microarray analysis using C2C12 myotubes that had been infected with adenovirus overexpressing SENP2 (Ad-SENP2). Remarkably, the mRNA levels of the proteins involved in the metabolic process of fatty acids (including ACSL1, CPT1b, and UCP3) as well as of glucose were dramatically upregulated (Fig. 3A). Interestingly, however, the mRNA levels of the proteins involved in cell cycle and DNA replication were markedly downregulated by SENP2 overexpression. These results indicated that SENP2 is functionally related to energy metabolism in myotubes.

For further confirmation of this finding, C2C12 myotubes were infected with Ad-SENP1, Ad-SENP2, and its catalytically inactive form (C548S) (Ad-SENP2mt) (Supplementary Fig. 4A and B). Consistent with the data from microarray analysis, overexpression of SENP2, but not SENP1 or SENP2mt, led to an increase in the mRNA levels of FAO-associated enzymes (Fig. 3B). Moreover, the increase in FAO by overexpression of SENP2 was significantly higher than that by overexpression of SENP1 or SENP2mt (Fig. 3C). On the other hand, overexpression of SENP2 showed little or no effect on the expression of mRNAs for transcription factors involved in lipid metabolism, such as PPAR α , PPAR δ , PPAR γ , PGC1 α , and estrogen-related receptor α (Supplementary Fig. 4C). These results suggest that the desumoylating activity of SENP2 is required for the promotion of FAO via upregulation of the expression of FAO-associated enzymes in C2C12 myotubes.

SENP2 Increases FAO Mainly by Promoting PPAR δ - and PPAR γ -Mediated Expression of FAO-Associated Enzymes

To determine whether SENP2-dependent increase in the expression of FAO-associated enzymes is mediated by

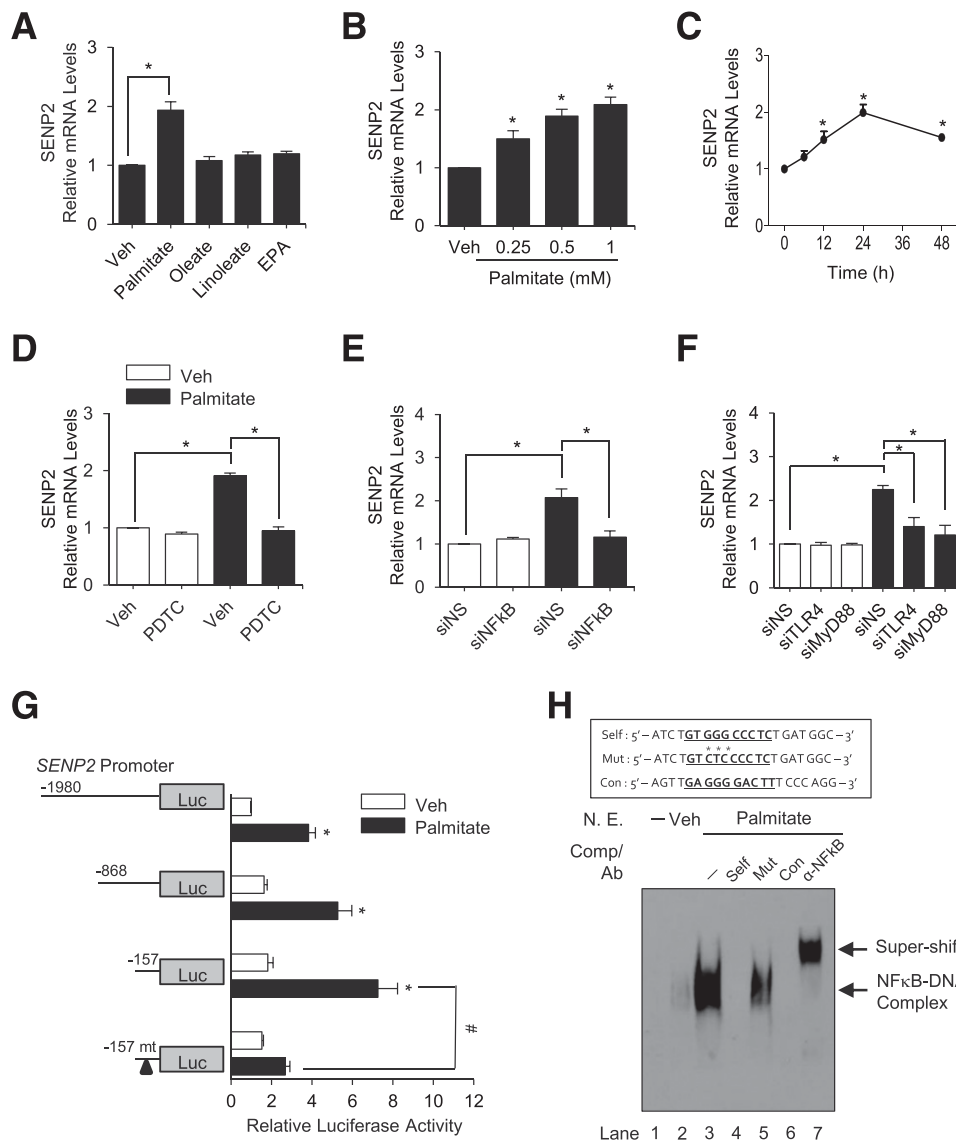


Figure 1—Expression of SENP2 mRNA is regulated by palmitate-induced NF-κB activation. **A:** C2C12 myotubes were treated with various fatty acids (0.5 mmol/L) for 24 h. Free fatty acids (100 mmol/L in EtOH) were diluted in the culture medium containing fatty acid-free BSA in a 1:3 molar ratio. The mRNA levels of SENP2 were then determined by real-time PCR. Each Ct value was subtracted by Ct value of GAPDH (Δ Ct) and then subtracted by the Δ Ct of each control set (ddCt). Relative mRNA levels were expressed as $2^{-\Delta\Delta Ct}$. The SENP2 mRNA level of untreated cells (vehicle [Veh]) was expressed as 1.0, and the others were expressed as its relative values. Data are the mean \pm SEM of five independent experiments. * $P < 0.05$. **B:** C2C12 myotubes were treated with increasing amounts of palmitate for 24 h ($n = 4$). * $P < 0.05$ compared with untreated cells (Veh). **C:** C2C12 myotubes were treated with 0.5 mmol/L palmitate for increasing periods and then subjected to assay for SENP2 mRNA levels ($n = 5$). * $P < 0.05$ compared with untreated cells. **D:** C2C12 myotubes were treated with palmitate in the absence or presence of 10 μ mol/L pyrrolidine dithiocarbamate ($n = 4$). * $P < 0.05$. **E:** C2C12 myotubes were transfected with siRNA against NF-κB (50 nmol/L) for 24 h and then treated with palmitate for 24 h ($n = 3$). * $P < 0.05$. **F:** C2C12 myotubes transfected with the indicated siRNAs were treated with palmitate ($n = 4$). * $P < 0.05$. **G:** C2C12 myoblasts were transfected with *Luc* reporter vectors harboring various deletions of promoter region in the *SENP2* gene. After treatment with palmitate for 24 h, they were subjected to assay for *Luc* activity ($n = 4$). The arrowhead indicates the mutations shown in **H**. The *Luc* activity of the cells transfected with (−1980)-*Luc* without palmitate was set to 1, and the other values were expressed relative to that. * $P < 0.05$ compared with untreated cells; # $P < 0.05$. **H:** The putative NF-κB-binding sequence in the *SENP2* promoter (−85 bp to −54 bp) is underlined in “Self.” The underline in “Con” (consensus) indicates the consensus NF-κB-binding sequence. *Mutated (Mut) bases (upper panel). Nuclear extracts were prepared from C2C12 myotubes that had been incubated without (Veh) and with palmitate for 24 h. They were then subjected to EMSA assay using a biotin-labeled probe (lower panel). For competition assays, unlabeled oligonucleotides (50-fold) (Self, Mut, and Con) were used as competitors (Comp). NF-κB antibody (Ab) was used for supershift. Lane 1 represented the probe only. siNS, nonspecific siRNA.

desumoylation of transcription factors that are involved in lipid metabolism, we first performed knockdown analysis of each of them. Supplementary Fig. 4D shows that each siRNA used effectively depletes the mRNA of its

target transcription factor (i.e., PPAR α , PPAR δ , PPAR γ , PGC1 α , estrogen-related receptor α , and receptor-interacting protein 140). Interestingly, knockdown of PPAR δ and PPAR γ , but not of the others, dramatically

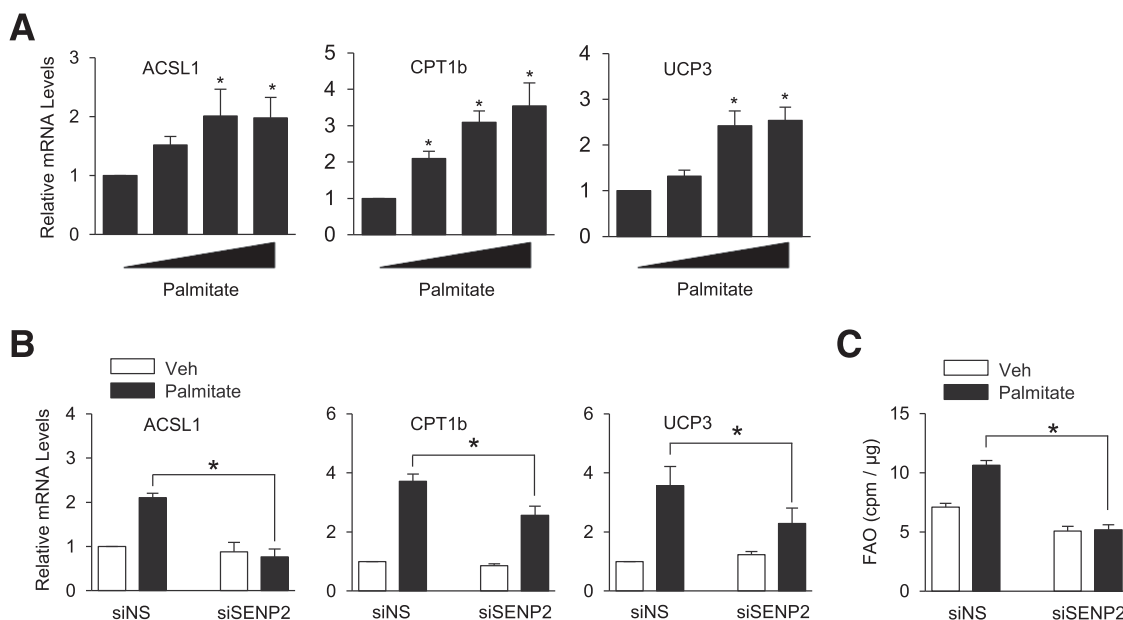


Figure 2—SENP2 is responsible for palmitate-mediated increase of FAO. **A:** Total RNAs were prepared from C2C12 myotubes that had been treated with 0.25, 0.5, or 1 mmol/L palmitate for 24 h. They were then subjected to real-time PCR ($n = 4$). * $P < 0.05$ compared with untreated cells. **B and C:** Myotubes were transfected with siRNAs against SENP2 (siSENP2). After incubation for 24 h, they were treated with 0.5 mmol/L palmitate ($n = 5$). The mRNA levels for the indicated proteins (**B**) and FAO (**C**) were then determined. siNS, nonspecific siRNA. * $P < 0.05$.

suppressed SENP2-mediated increase in the mRNA levels of FAO-associated enzymes and thereby in FAO (Fig. 3D and E, respectively). On the other hand, the basal FAO level in the absence of SENP2 overexpression was not influenced by knockdown of any of the transcription factors, including PPAR δ and PPAR γ (Supplementary Fig. 4E). These results suggest that SENP2 increases FAO mainly by promoting PPAR δ - and PPAR γ -mediated expression of FAO-associated enzymes.

For determination of whether SENP2 influences the recruitment of PPAR δ and PPAR γ to the promoters of their target genes for the control of FAO, chromatin immunoprecipitation-coupled quantitative real-time PCR analysis (ChIP-qPCR) was performed using C2C12 myotubes that had been transfected with Ad-GFP, Ad-SENP2, and Ad-SENPmt. Overexpression of SENP2, but not SENP2mt, markedly promoted the binding of PPAR δ and PPAR γ to the *CPT1b* promoter region, whereas it showed little or no effect on that of PPAR α and PGC1 α (Fig. 3F). Similar results were obtained using the *ACSL1* promoter region (Fig. 3G). These results indicate that SENP2 increases mRNA expression of FAO-associated enzymes by promoting the recruitment of PPAR δ and PPAR γ to the promoters of the genes.

Next, we tested whether palmitate-induced mRNA level increase of FAO-associated enzymes was also mediated by PPAR δ and PPAR γ recruitment to their promoters and whether SENP2 was involved in the process. The recruitment of PPAR δ and PPAR γ to the *CPT1b* or *ACSL1* promoters was increased by palmitate and knockdown of SENP2 suppressed the effect of palmitate (Fig. 3H and I).

These results suggest that SENP2 plays an important role in the palmitate-induced recruitment of PPAR δ and PPAR γ to the promoters of the FAO-associated enzyme genes.

SENP2 Promotes PPAR δ Activity by Desumoylation

We have previously shown that SENP2 desumoylates PPAR γ and promotes its activity (32). To determine whether PPAR δ also is a target for SENP2, we first examined whether PPAR δ is sumoylated. Sequence analysis revealed that PPAR δ contains the MK¹⁰⁴LE sequence, which is conserved in mouse and human and similar to the consensus sumoylation Ψ KXE motif, where Ψ is a hydrophobic amino acid and X is any amino acid (Fig. 4A). Therefore, we replaced the Lys¹⁰⁴ residue with Arg to test whether the mutation (K104R) influences PPAR δ sumoylation. Overexpression of SUMO1 and UBC9 (sumoylation E2 enzyme) with PPAR δ , but not with its K104R mutant, dramatically increased the appearance of slow-migrating PPAR δ bands (Fig. 4B). Furthermore, the slow-migrating bands could completely be eliminated by the expression of SENP2 but not by SENP2mt (Fig. 4C). These results indicate that PPAR δ , like PPAR γ , serves as a target of SENP2 and its Lys¹⁰⁴ residue is a major SUMO acceptor site. The higher-molecular weight bands were also detected with anti-ubiquitin antibody as well as anti-SUMO antibody, and ubiquitination of PPAR δ was increased when sumoylation was accompanied (Supplementary Fig. 5A). Therefore, it is possible that sumoylation of PPAR δ promotes ubiquitination, which generates multiple high-molecular weight bands. We also confirmed desumoylation of endogenous PPAR δ by SENP2 overexpression in myotubes (Supplementary Fig. 5B).

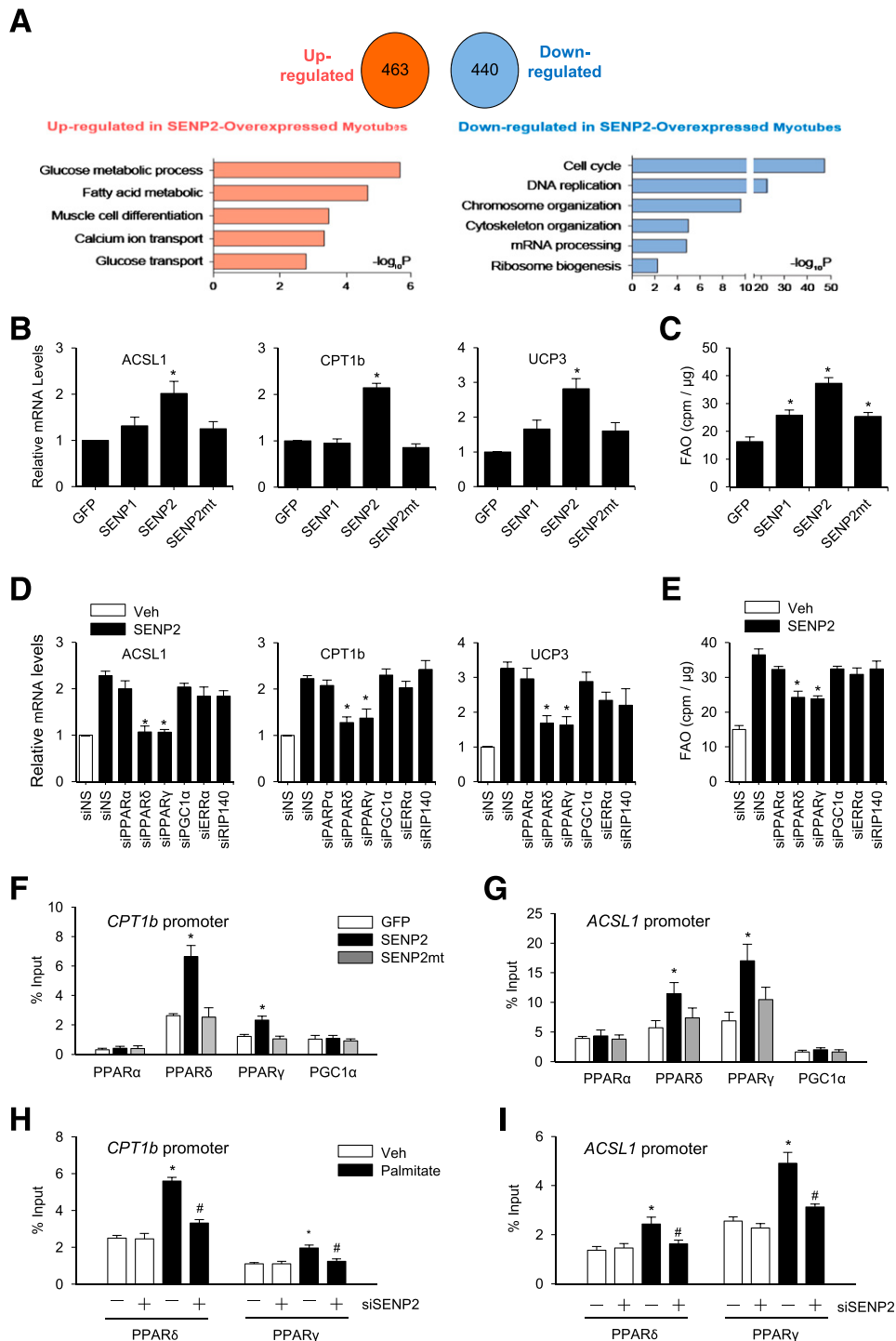


Figure 3—SENP2 increases FAO by promoting PPAR δ - and PPAR γ -mediated expression of FAO-associated enzymes. **A**: Total RNA was isolated from C2C12 myotubes that had been infected with Ad-GFP or Ad-SENP2 for 3 days and then subjected to microarray. Differentially expressed genes were identified as those with false discovery rates <0.05 and fold change larger than the cutoff of 1.5. **B**: C2C12 myotubes were infected with Ad-GFP, Ad-SENP1, Ad-SENP2, or Ad-SENP2mt for 3 days. Total RNAs were obtained from the cells and then subjected to real-time PCR ($n = 4$). **C**: Cells prepared as in **B** were subjected to FAO assay ($n = 5$). * $P < 0.05$ compared with Ad-GFP infected cells. **D** and **E**: C2C12 myotubes transfected with the indicated siRNAs were infected with Ad-GFP or Ad-SENP2. siNS, nonspecific siRNA. After incubation for 48 h, the mRNA levels of FAO-associated enzymes ($n = 4$) and FAO ($n = 6$) were determined. * $P < 0.05$ compared with cells transfected with nonspecific siRNA and Ad-SENP2. **F** and **G**: C2C12 myotubes infected with Ad-GFP, Ad-SENP2, or Ad-SENP2mt were subjected to ChIP-qPCR analysis with the *CPT1b* promoter region (**F**) and *ACSL1* promoter region (**G**). Data are the means \pm SEM ($n = 4$). * $P < 0.05$ compared with Ad-GFP-infected cells. **H** and **I**: C2C12 myotubes were treated with siSENP2 for 24 h followed by treatment of palmitate (500 μ mol/L) for 24 h and then subjected to ChIP-qPCR ($n = 3$). Veh, vehicle. * $P < 0.05$ compared with nonspecific siRNA without palmitate. # $P < 0.05$ compared with nonspecific siRNA with palmitate.

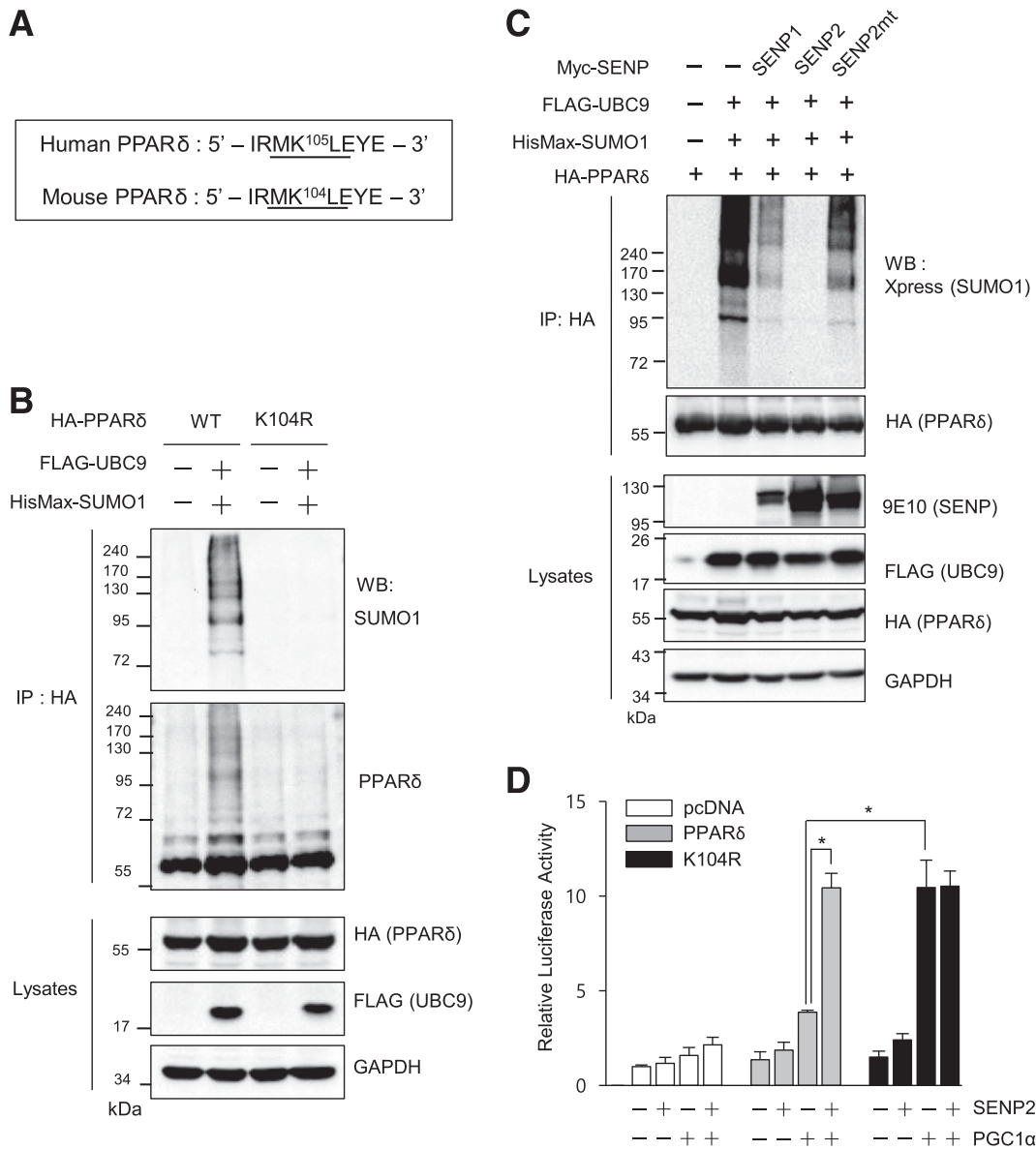


Figure 4—SENP2 promotes the PPAR δ activity by desumoylation. **A**: The putative sumoylation sequences of human and mouse PPAR δ are shown. **B**: HA-tagged PPAR δ and its K104R mutant were expressed in MCF7 cells with HisMax-SUMO1 and FLAG-UBC9. Cell lysates were subjected to immunoprecipitation (IP) with anti-HA antibody followed by Western blotting (WB) with anti-SUMO1 and anti-PPAR δ antibodies. Cell lysates were also directly probed with the indicated antibodies. **C**: HA-PPAR δ , HisMax-SUMO1, and FLAG-UBC9 were expressed with Myc-tagged SENP1 or SENP2 or its mutant (SENP2mt). Immunoprecipitation was then carried out as in **B**. **D**: COS7 cells were treated with siRNAs (50 nmol/L) against PPAR γ to minimize the effect of endogenous PPAR γ . The following day, cells were transfected with pPPRE-TK-Luc and expression vectors of SENP2, PGC1 α , PPAR δ , or PPAR δ K104R. Luc activity of cells transfected with pPPRE-TK-Luc only was expressed as 1.0, and the others were expressed as its relative values ($n = 4$). * $P < 0.05$.

For examination of whether PPAR δ sumoylation affects its activity, COS7 cells were transfected with a pPPRE-TK-Luc reporter vector. Note that coexpression of PGC1 α was necessary to detect the PPAR δ activity in nonmuscle COS7 cells, which were used instead of C2C12 myotubes having very low transfection efficiency. Overexpression of SENP2 dramatically increased the activity of PPAR δ (Fig. 4D). Remarkably, the activity of sumoylation-deficient K104R seen without SENP2 was nearly as high as that of wild-type (WT) PPAR δ seen with SENP2, indicating that SENP2-mediated

desumoylation is required for PPAR δ to show its maximal activity. Taken together, these results indicate that SENP2 promotes the activity of PPAR δ as well as PPAR γ through desumoylation.

SENP2 Overexpression in Muscle Ameliorates High-Fat Diet-Induced Obesity and Insulin Resistance

To determine whether SENP2 is indeed involved in lipid metabolism in vivo, we generated muscle-specific SENP2 transgenic mice (referred to as mSENP2-TG mice) by inserting the SENP2-FLAG construct to a β -globin gene

cassette having the *MCK* promoter (Supplementary Fig. 6A). The *SENP2* mRNA was expressed in all types of muscle tissues of mSENP2-TG mice but not in those of WT mice (Supplementary Fig. 6B). It was not expressed in the liver or epididymal fat tissues of both the TG and WT mice (Supplementary Fig. 6C). Consistently, the *SENP2* protein could be detected in the skeletal muscle of the TG mice but not in that of WT mice (Supplementary Fig. 6D). In addition, the total protein level of *SENP2* (i.e., FLAG-tagged and endogenous *SENP2*) was at least three- to fourfold higher in the muscle of mSENP2-TG mice than that of WT mice under both chow- and high-fat diet (HFD)-fed conditions (Supplementary Fig. 6E). These results confirmed that the TG mice overexpress *SENP2* in muscle.

Remarkably, the body weight and fat mass of mSENP2-TG mice were significantly lower than those of WT mice under HFD-fed conditions, whereas lean mass and bone mineral contents of the TG mice were similar to that of WT mice (Fig. 5A–D). Analysis by glucose tolerance tests and insulin tolerance tests revealed that mSENP2-TG mice show higher glucose tolerance and insulin sensitivity than WT mice under HFD-fed conditions (Fig. 5E and F). Moreover, the basal levels of insulin and triglyceride in the serum of HFD-fed TG mice were much lower than those of WT mice (Fig. 5G and H). On the other hand, little or no difference was detected in the serum cholesterol level under both chow- and HFD-fed conditions (Fig. 5I). Moreover, electron microscopic analysis revealed that the gastrocnemius muscle of the TG mice contained much lower fat than that of WT mice under HFD-fed conditions (Fig. 5J). On the other hand, the fat level in the liver and fat size of adipose tissues of the TG mice was similar to that of WT mice under both chow- and HFD-fed conditions (Supplementary Fig. 7A and B). Significantly, insulin-stimulated phosphorylation of insulin receptor substrate 1 and protein kinase B (PKB/Akt) in the gastrocnemius muscle of mSENP2-TG mice was much higher than that of WT mice under both chow- and HFD-fed conditions (Fig. 5K), suggesting that *SENP2* promotes insulin signaling. Taken together, these results indicate that *SENP2* overexpression in muscle alleviates HFD-induced obesity and insulin resistance.

SENP2 Overexpression Increases FAO by Upregulating Expression of FAO-Associated Enzymes in Muscle

Next, we determined the levels of free fatty acids and triglyceride in the gastrocnemius muscle. While the level of free fatty acids in the muscle tissue of the TG mice was similar to that of WT mice (Fig. 6A), the triglyceride level in the TG mice was significantly lower than that of WT mice under both chow- and HFD-fed conditions (Fig. 6B). In addition, FAO was markedly increased in the muscle of the TG mice under both chow- and HFD-fed conditions compared with that of WT mice (Fig. 6C), and ATP contents were also increased in the muscle of HFD-fed TG mice (Supplementary Fig. 7C). These results indicate that

the muscle tissues of the TG mice show higher FAO, which would reduce fat accumulation.

We next examined whether the increase in FAO is associated with *SENP2*-mediated changes in the expression of FAO-associated enzymes (i.e., *ACSL1*, *CPT1b*, and *UCP3*). Consistent with the results obtained with cell culture system, the mRNA levels of FAO-associated enzymes were higher in the gastrocnemius muscle of HFD-fed TG mice than in that of WT mice (Fig. 6D). In contrast, in the muscle of chow-fed TG mice, only *UCP3* mRNA, but not *ACSL1* or *CPT1b* mRNA, levels were increased (Fig. 6D). When the mRNA levels of these FAO-associated enzymes of the WT mice muscle were compared under different diet conditions, the levels were similar in chow- and HFD conditions (Fig. 6D), and *SENP2* mRNA levels of the WT mice were not significantly affected by diet condition, either (Supplementary Fig. 7D). In addition, no apparent difference between mSENP2-TG and WT mice muscles was observed in the mRNA levels of transcriptional factors, including *PPAR α* , *PPAR δ* , *PPAR γ* , and *PGC1 α* in both chow- and HFD-fed conditions (Fig. 6E). Collectively, these results suggest that *SENP2* plays a critical role in the increase of FAO by inducing the expression of FAO-related enzymes and *SENP2* overexpression in muscle alleviates HFD-induced obesity and insulin resistance.

DISCUSSION

On the basis of the present findings, we propose a potential mechanism by which *SENP2* regulates lipid metabolism in skeletal muscle (Fig. 7). Upon saturated free fatty acid stimulation, *TLR4/MyD88* activates *NF- κ B* for expression of *SENP2* transcripts, which would increase the cellular level of *SENP2* protein. This increase leads to desumoylation of *PPAR δ* and *PPAR γ* and their recruitment to the promoters of the genes encoding FAO-associated enzymes, including *ASCL1* and *CPT1b*. Elevated expression of the enzymes would then promote FAO (the upper panel). In the muscle of mSENP2-TG mice, overexpressed *SENP2* increases FAO via the same mechanism described above but without the need of the signal from saturated fatty acids. This increase in FAO then results in fat utilization and suppression of its accumulation, which alleviates HFD-induced obesity and insulin resistance (the lower panel). These findings demonstrate that *SENP2* serves as an important regulator of lipid metabolism in muscle.

Several questions may be raised from our data and model. A question is why *SENP2*-induced FAO is not observed in HFD-fed WT mice. In an *in vitro* C2C12 myotube culture system, palmitate treatment significantly increases *SENP2* expression, which increases FAO. In contrast, *SENP2* expression is not substantially increased in the muscle of HFD-fed mice (Supplementary Figs. 6E and 7D). Similarly, either FAO or the mRNA levels of *ACSL1* and *CPT1b* are not significantly changed by HFD (Fig. 6C and D). The different results in these models could derive from other metabolic disturbances associated with chronic high-fat feeding or from different experimental systems (*in vitro* vs. *in vivo*).

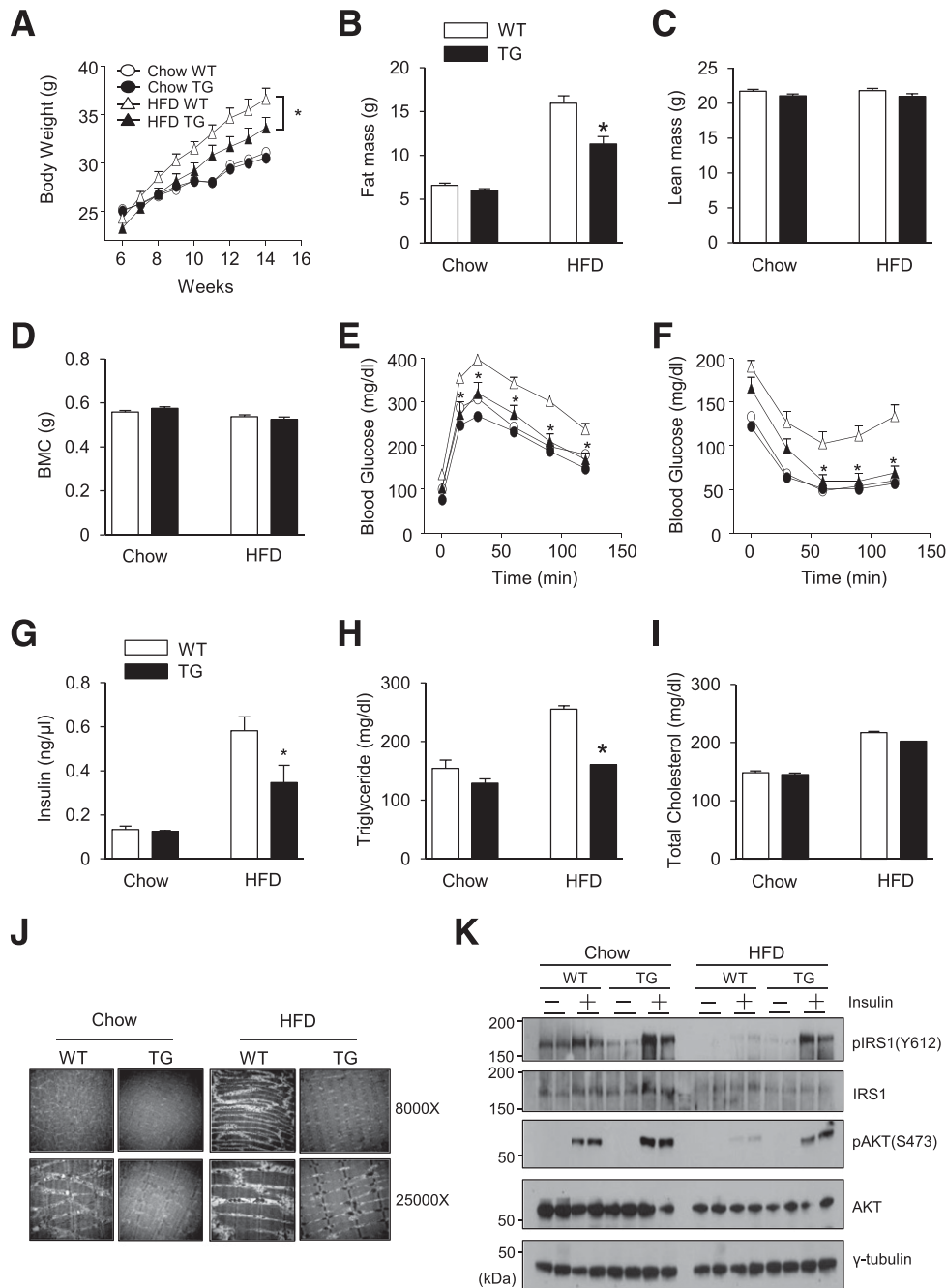


Figure 5—Muscle-specific SENP2 overexpression alleviates HFD-induced obesity and insulin resistance. **A**: WT and mSENP2-TG (TG) mice at 8 weeks were fed with a standard chow diet or HFD, consisting of 60% fat and 6.8% sucrose, for the next 12 weeks. Their body weights were measured every day for 14 weeks ($n = 15\text{--}20/\text{group}$). Data are the mean \pm SEM. $*P < 0.05$. **B–D**: Body fat mass (**B**), lean mass (**C**), and bone mineral contents (BMC) (**D**) were measured after feeding the mice with chow or HFD for 10 weeks using DXA scanning. $*P < 0.05$. **E** and **F**: Glucose tolerance test (**E**) and insulin tolerance test (**F**) were performed. $*P < 0.05$. **G–I**: The levels of insulin (**G**), triglycerides (**H**), and total cholesterol (**I**) in serum were measured. $*P < 0.05$. Note that the P values were in comparison with WT mice fed with HFD (**B** and **E–H**). **J**: Sections of gastrocnemius muscle tissues were obtained and then subjected to electron microscopy. **K**: Mice were treated with insulin for 20 min before sacrifice. Extracts prepared from the gastrocnemius muscle were subjected to immunoblot with respective antibodies.

It is notable that the mRNA levels of UCP3 are higher in the muscle of chow-fed SENP2-TG mice, but unexpectedly the mRNA levels of ACSL1 and CPT1b are not increased (Fig. 6D). These are different from the data observed in the myotube culture system. Given that the source of fatty acids available for FAO in the chow-

fed condition is limited, it is conceivable that a certain level of fatty acid could be required for inducing ACSL1 and CPT1b gene expression. Additionally, a yet unidentified regulatory system that may suppress ACSL1 or CPT1b expression independently of SENP2 in the context of in vivo milieu is possibly involved in this event.

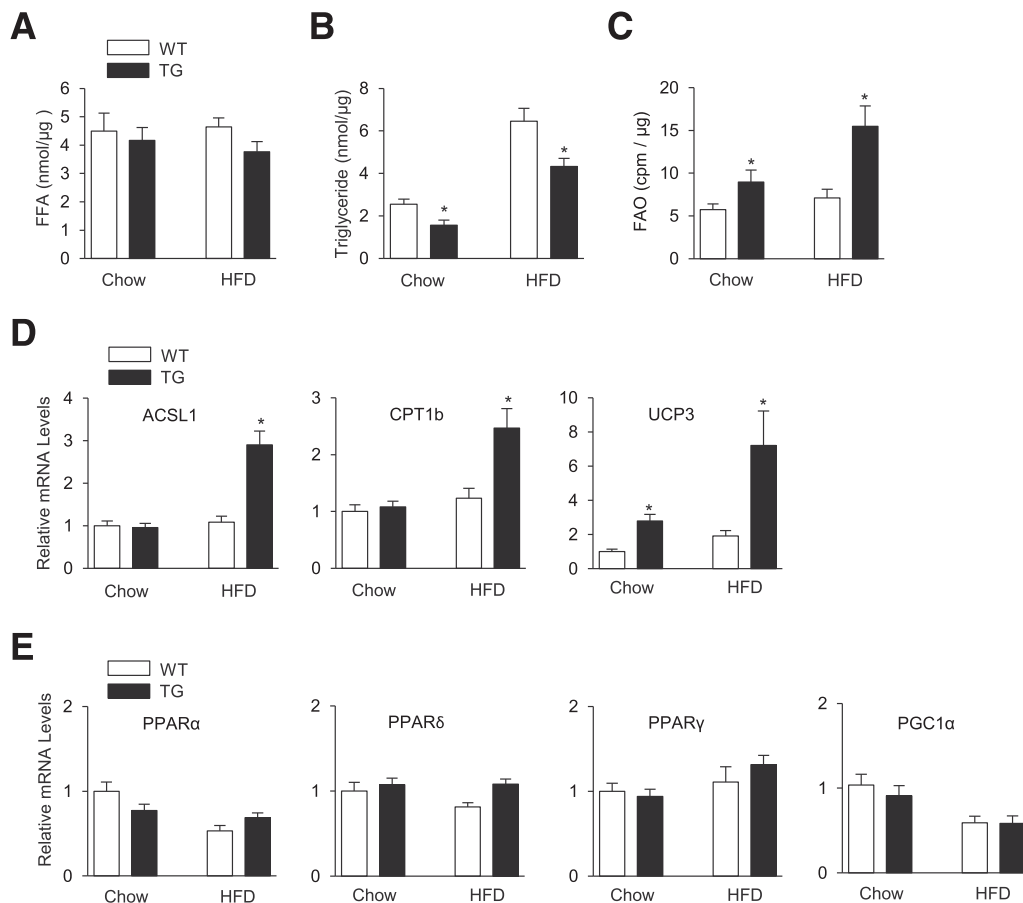


Figure 6—SENP2 overexpression increases FAO by upregulating expression of FAO-associated enzymes in muscle. *A–C*: WT and mSENP2-TG (TG) mice were fed with chow or HFD for 12 weeks. The levels of free fatty acids (FFA) (*A*), triglycerides (*B*), and FAO (*C*) in their gastrocnemius muscle were determined ($n = 8/\text{group}$). *D* and *E*: Total mRNAs were isolated from the muscles of the mice and subjected to real-time PCR ($n = 10\text{--}14/\text{group}$) using primers for FAO-associated enzymes (*D*) and PPARs and PGC1 α (*E*). The mRNA level seen in chow-fed WT mice muscle was expressed as 1.0, and the others were expressed as its relative values. Data are the mean \pm SEM. * $P < 0.05$ compared with WT mice.

Future studies will need to clarify these important issues.

Another question is whether PPAR δ and PPAR γ are only direct targets of SENP2 to promote FAO in muscle. The effect of palmitate on FAO is completely abolished by SENP2 knockdown, while knockdown of SENP2 partially inhibits palmitate-induced expression of CPT1b and UCP3 (Fig. 2*B* and *C*), although CPT1 is known to be the limiting step of FAO. In addition, knockdown of PPAR δ or PPAR γ efficiently, but not completely, suppresses SENP2-mediated FAO (Fig. 3*E*). These observations indicate the possibility that SENP2 regulates the function of FAO-associated enzymes through direct modification, at least in part. It is also possible that SENP2 controls the expression or function of another protein(s) that is important for FAO but not tested in this study. Nevertheless, our study clearly shows that SENP2 increases FAO mainly by promoting PPAR δ - and PPAR γ -mediated expression of FAO-associated enzymes.

While sumoylation of PPAR γ was previously reported, to our knowledge, we show for the first time that

PPAR δ is sumoylated. Of note was the finding that high-molecular weight sumoylated bands of PPAR δ were detected (Fig. 4*B* and *C*). However, it is unlikely that PPAR δ is sumoylated at multiple sites because its K104R mutation completely abrogated PPAR δ sumoylation. The fact that SUMO1 is known to be incapable of forming a polymeric chain and our result showing that ubiquitination of PPAR δ is increased by sumoylation suggest that the high-molecular weight bands consist of PPAR δ modified by both SUMO1 and ubiquitin. In fact, there are several reports that sumoylation of proteins promotes their ubiquitination (42–44). Further study will determine whether the ubiquitination is linked to proteasome-mediated degradation of PPAR δ .

PPAR δ is more abundant than PPAR γ in muscle, suggesting that the contribution of PPAR δ in lipid metabolism in muscle could be greater than that of PPAR γ . Interestingly, however, the effect of PPAR γ on gene expression of FAO-associated enzymes and in turn on FAO in C2C12 myotubes was nearly similar to that of PPAR δ (Fig. 3*D* and *E*). Thus, it appears that PPAR γ , in addition

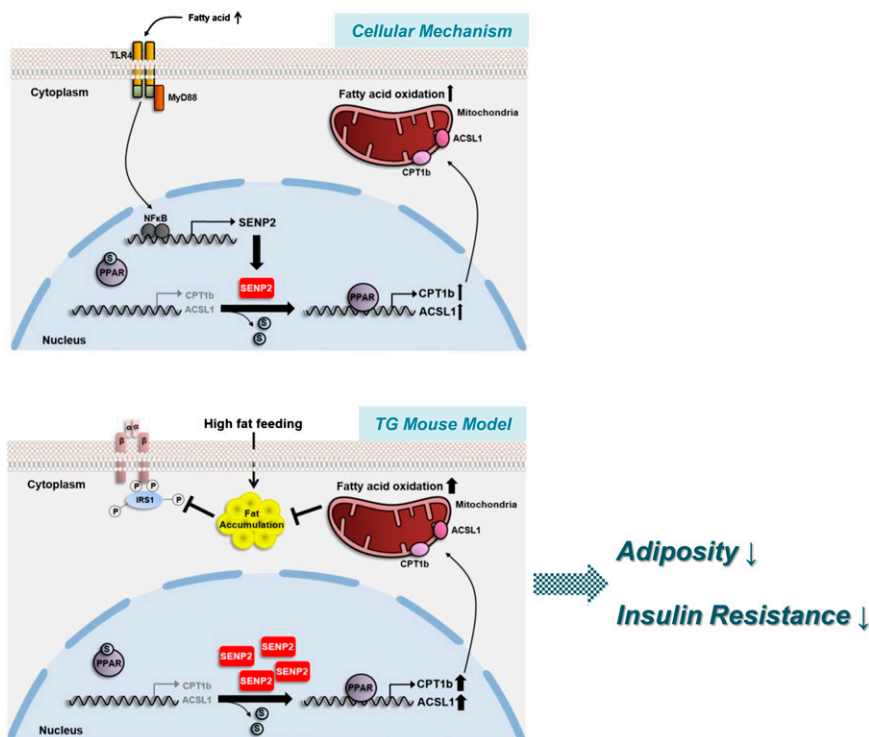


Figure 7—Schematic model shows the role of SENP2 in the control of lipid metabolism in skeletal muscle. Upon sensing by saturated free fatty acids, TLR4/MyD88 activates NF- κ B for expression of SENP2 mRNA, which would increase the cellular level of SENP2 protein for desumoylation of PPAR δ and PPAR γ . These transcription factors are then recruited to the promoters of the genes encoding FAO-associated enzymes, such as ACSL1 and CPT1b, which leads to increase of FAO (the upper panel). Muscle-specific overexpression of SENP2 in TG mice increases the expression of FAO-associated enzymes and thereby increases FAO. This increase would elevate fat utilization and suppress its accumulation, which could alleviate HFD-induced obesity and insulin resistance (lower panel). S, SUMO.

to PPAR δ , plays an important role in lipid metabolism in skeletal muscle. This is further supported by experimental evidence showing that muscle-specific deletion of PPAR γ results in insulin resistance and promotes adiposity (45,46).

Acknowledgments. The authors thank Dr. C.H. Chung (Seoul National University) for helpful discussion during preparation of the manuscript.

Funding. This research was supported by Basic Science Research Program through the National Research Foundation of Korea (NRF) funded by the Ministry of Education, Science and Technology (MEST) (2012R1A1A2008894), a NRF grant funded by the Korean government (MEST) (2006-2005410), a grant from the Seoul National University Hospital (03-2011-0150), and a grant from the National Institutes of Health (1R01DK083567 to Y.-B.K.). This work was also supported by Protein Metabolism Medical Research Center through the Seoul National University Nobel Laureates Invitation Program.

Duality of Interest. No potential conflicts of interest relevant to this article were reported.

Author Contributions. Y.D.K., J.W.C., My.K., S.C., B.Y.A., Mi.K., and B.C.O. performed experiments and analyzed data. Y.D.K., S.S.C., and K.S.P. wrote the manuscript. D.H., J.H.S., Y.-B.K., Y.J.P., S.S.C., and K.S.P. contributed to discussion and reviewed and edited the manuscript. Y.D.K., S.S.C., and K.S.P. are the guarantors of this work and, as such, had full access to all the data in the study and take responsibility for the integrity of the data and the accuracy of the data analysis.

References

1. Pan DA, Lillioja S, Kriketos AD, et al. Skeletal muscle triglyceride levels are inversely related to insulin action. *Diabetes* 1997;46:983–988

2. Perseghin G, Scifo P, De Cobelli F, et al. Intramyocellular triglyceride content is a determinant of in vivo insulin resistance in humans: a ^1H - ^{13}C nuclear magnetic resonance spectroscopy assessment in offspring of type 2 diabetic parents. *Diabetes* 1999;48:1600–1606

3. Jacob S, Machann J, Rett K, et al. Association of increased intramyocellular lipid content with insulin resistance in lean nondiabetic offspring of type 2 diabetic subjects. *Diabetes* 1999;48:1113–1119

4. Krssak M, Falk Petersen K, Dresner A, et al. Intramyocellular lipid concentrations are correlated with insulin sensitivity in humans: a ^1H NMR spectroscopy study. *Diabetologia* 1999;42:113–116

5. Schmitz-Peiffer C, Craig DL, Biden TJ. Ceramide generation is sufficient to account for the inhibition of the insulin-stimulated PKB pathway in C2C12 skeletal muscle cells pretreated with palmitate. *J Biol Chem* 1999;274:24202–24210

6. Bruce CR, Hoy AJ, Turner N, et al. Overexpression of carnitine palmitoyltransferase-1 in skeletal muscle is sufficient to enhance fatty acid oxidation and improve high-fat diet-induced insulin resistance. *Diabetes* 2009;58:550–558

7. Choi CS, Savage DB, Abu-Elheiga L, et al. Continuous fat oxidation in acetyl-CoA carboxylase 2 knockout mice increases total energy expenditure, reduces fat mass, and improves insulin sensitivity. *Proc Natl Acad Sci U S A* 2007;104:16480–16485

8. Perdomo G, Commerford SR, Richard AM, et al. Increased beta-oxidation in muscle cells enhances insulin-stimulated glucose metabolism and protects against fatty acid-induced insulin resistance despite intramyocellular lipid accumulation. *J Biol Chem* 2004;279:27177–27186

9. Feige JN, Lagogue M, Canto C, et al. Specific SIRT1 activation mimics low energy levels and protects against diet-induced metabolic disorders by enhancing fat oxidation. *Cell Metab* 2008;8:347–358

10. Willson TM, Brown PJ, Sternbach DD, Henke BR. The PPARs: from orphan receptors to drug discovery. *J Med Chem* 2000;43:527–550

11. Kleiner S, Nguyen-Tran V, Baré O, Huang X, Spiegelman B, Wu Z. PPARdelta agonism activates fatty acid oxidation via PGC-1alpha but does not increase mitochondrial gene expression and function. *J Biol Chem* 2009;284:18624–18633
12. Tontonoz P, Hu E, Spiegelman BM. Stimulation of adipogenesis in fibroblasts by PPAR gamma 2, a lipid-activated transcription factor. *Cell* 1994;79:1147–1156
13. Johnson ES. Protein modification by SUMO. *Annu Rev Biochem* 2004;73:355–382
14. Hay RT. SUMO: a history of modification. *Mol Cell* 2005;18:1–12
15. Geiss-Friedlander R, Melchior F. Concepts in sumoylation: a decade on. *Nat Rev Mol Cell Biol* 2007;8:947–956
16. Zhao J. Sumoylation regulates diverse biological processes. *Cell Mol Life Sci* 2007;64:3017–3033
17. Hay RT. SUMO-specific proteases: a twist in the tail. *Trends Cell Biol* 2007;17:370–376
18. Mukhopadhyay D, Dasso M. Modification in reverse: the SUMO proteases. *Trends Biochem Sci* 2007;32:286–295
19. Hickey CM, Wilson NR, Hochstrasser M. Function and regulation of SUMO proteases. *Nat Rev Mol Cell Biol* 2012;13:755–766
20. Yeh ET. SUMOylation and De-SUMOylation: wrestling with life's processes. *J Biol Chem* 2009;284:8223–8227
21. Cheng J, Kang X, Zhang S, Yeh ET. SUMO-specific protease 1 is essential for stabilization of HIF1alpha during hypoxia. *Cell* 2007;131:584–595
22. Chiu SY, Asai N, Costantini F, Hsu W. SUMO-specific protease 2 is essential for modulating p53-Mdm2 in development of trophoblast stem cell niches and lineages. *PLoS Biol* 2008;6:e310
23. Kang X, Qi Y, Zuo Y, et al. SUMO-specific protease 2 is essential for suppression of polycomb group protein-mediated gene silencing during embryonic development. *Mol Cell* 2010;38:191–201
24. Bawa-Khalife T, Cheng J, Wang Z, Yeh ET. Induction of the SUMO-specific protease 1 transcription by the androgen receptor in prostate cancer cells. *J Biol Chem* 2007;282:37341–37349
25. Cheng J, Bawa T, Lee P, Gong L, Yeh ET. Role of desumoylation in the development of prostate cancer. *Neoplasia* 2006;8:667–676
26. Han Y, Huang C, Sun X, et al. SENP3-mediated de-conjugation of SUMO2/3 from promyelocytic leukemia is correlated with accelerated cell proliferation under mild oxidative stress. *J Biol Chem* 2010;285:12906–12915
27. Lee MH, Lee SW, Lee EJ, et al. SUMO-specific protease SUSP4 positively regulates p53 by promoting Mdm2 self-ubiquitination. *Nat Cell Biol* 2006;8:1424–1431
28. Tang S, Huang G, Tong X, et al. Role of SUMO-specific protease 2 in reprogramming cellular glucose metabolism. *PLoS ONE* 2013;8:e63965
29. Cai R, Yu T, Huang C, et al. SUMO-specific protease 1 regulates mitochondrial biogenesis through PGC-1alpha. *J Biol Chem* 2012;287:44464–44470
30. Yamashita D, Yamaguchi T, Shimizu M, Nakata N, Hirose F, Osumi T. The transactivating function of peroxisome proliferator-activated receptor gamma is negatively regulated by SUMO conjugation in the amino-terminal domain. *Genes Cells* 2004;9:1017–1029
31. Rytinki MM, Palvimo JJ. SUMOylation attenuates the function of PGC-1alpha. *J Biol Chem* 2009;284:26184–26193
32. Chung SS, Ahn BY, Kim M, Kho JH, Jung HS, Park KS. SUMO modification selectively regulates transcriptional activity of peroxisome-proliferator-activated receptor gamma in C2C12 myotubes. *Biochem J* 2011;433:155–161
33. Chung SS, Ahn BY, Kim M, et al. Control of adipogenesis by the SUMO-specific protease SENP2. *Mol Cell Biol* 2010;30:2135–2146
34. Maloney E, Sweet IR, Hockenbery DM, et al. Activation of NF-kappaB by palmitate in endothelial cells: a key role for NADPH oxidase-derived superoxide in response to TLR4 activation. *Arterioscler Thromb Vasc Biol* 2009;29:1370–1375
35. Cheng AM, Handa P, Tateya S, et al. Apolipoprotein A-I attenuates palmitate-mediated NF-kB activation by reducing Toll-like receptor-4 recruitment into lipid rafts. *PLoS ONE* 2012;7:e33917
36. Tsukumo DM, Carvalho-Filho MA, Carnevali JB, et al. Loss-of-function mutation in Toll-like receptor 4 prevents diet-induced obesity and insulin resistance. *Diabetes* 2007;56:1986–1998
37. Kleinridders A, Schenten D, Köner AC, et al. MyD88 signaling in the CNS is required for development of fatty acid-induced leptin resistance and diet-induced obesity. *Cell Metab* 2009;10:249–259
38. McGarry JD, Brown NF. The mitochondrial carnitine palmitoyltransferase system. From concept to molecular analysis. *Eur J Biochem* 1997;244:1–14
39. Ellis JM, Li LO, Wu PC, et al. Adipose acyl-CoA synthetase-1 directs fatty acids toward beta-oxidation and is required for cold thermogenesis. *Cell Metab* 2010;12:53–64
40. MacLellan JD, Gerrits MF, Gowing A, Smith PJ, Wheeler MB, Harper ME. Physiological increases in uncoupling protein 3 augment fatty acid oxidation and decrease reactive oxygen species production without uncoupling respiration in muscle cells. *Diabetes* 2005;54:2343–2350
41. Nabben M, Hoeks J. Mitochondrial uncoupling protein 3 and its role in cardiac- and skeletal muscle metabolism. *Physiol Behav* 2008;94:259–269
42. Tatham MH, Geoffroy MC, Shen L, et al. RNF4 is a poly-SUMO-specific E3 ubiquitin ligase required for arsenic-induced PML degradation. *Nat Cell Biol* 2008;10:538–546
43. van Hagen M, Overmeer RM, Abolvardi SS, Vertegaal AC. RNF4 and VHL regulate the proteasomal degradation of SUMO-conjugated Hypoxia-Inducible Factor-2alpha. *Nucleic Acids Res* 2010;38:1922–1931
44. Chen SC, Chang LY, Wang YW, et al. Sumoylation-promoted enterovirus 71 3C degradation correlates with a reduction in viral replication and cell apoptosis. *J Biol Chem* 2011;286:31373–31384
45. Hevener AL, He W, Barak Y, et al. Muscle-specific Pparg deletion causes insulin resistance. *Nat Med* 2003;9:1491–1497
46. Norris AW, Chen L, Fisher SJ, et al. Muscle-specific PPARgamma-deficient mice develop increased adiposity and insulin resistance but respond to thiazolidinediones. *J Clin Invest* 2003;112:608–618